

Local Acoustic Resonance Spectroscopy (LARS) for Glass Fiber-Reinforced Polymer Applications

Anne Jüngert · Christian Große · Markus Krüger

Received: 9 April 2013 / Accepted: 30 August 2013 / Published online: 3 December 2013
© Springer Science+Business Media New York 2013

Abstract Polymer composite materials combine high strength with low weight. This makes composites an interesting material for different industrial applications. In the aerospace industry, the use of composites is already common practice, while in the automotive industry carbon fiber-reinforced polymers have begun to replace metal in some parts. However, the nature of damage within composites is different from that within metal parts, so common techniques available for damage detection in metal may not work for composites thus new techniques for damage detection need to be developed. A technique that is often used but requires experienced technicians is the so-called coin tapping test where changes in sound waves generated by the impact of a hard object are detected. LARS is a (new) technique that avoids the errors due to variations in operator technique by using a instrumented impact device to generate controlled sound signals. If a hammer is used as an impact device it could be equipped with a dynamic force sensor to measure and record the excitation force of the sound signal. The force and the excited sound signal are related to the contact stiffness between the hammer and the test part. Flaws such as voids and delaminations affect the contact stiffness and can be detected under certain conditions. To the knowledge of the authors, no such technique has appeared in the literature. In regard to the frequencies, LARS is operated at much shorter wavelengths than in vibration analysis techniques (making it “local”) and at much larger wavelengths than in

ultrasound. The material is excited to frequencies that are recorded by a microphone. To demonstrate the method, it is applied to the inspection of wind turbine rotor blades.

Keywords Tap test · Local resonance · Plastic composites · Wind turbine blades

1 Introduction

The formation of voids within materials or between material layers is a known problem in different branches of industry. Composite materials especially tend to form cavities and delaminations due to the combination of different materials. There are several non-destructive testing techniques using, for example, ultrasound to detect voids within different materials. However, it is difficult to detect flaws with ultrasonic techniques in materials with high ultrasonic attenuation. The high attenuation necessitates the use of high energy pulses and low transducer frequencies. The resolution of ultrasonic inspection depends on the frequencies used. Some components contain materials with a high degree of damping so ultrasonic waves cannot propagate through them. The pulse-echo technique requires the identification of the defect echo. Shallow defects (like delaminations) are often camouflaged by the emitted pulse, and upper material layers cannot be tested at all.

In aerospace applications, simple coin tapping tests are used to detect these shallow flaws within composites. A hard item such as a coin is used to tap the surface. The location of delaminations can be determined by the registration of a hollow sound. As will be shown, this technique can be performed using a microphone to record the excited sound. A Fourier analysis of the sound is conducted whereby

A. Jüngert (✉) · M. Krüger
MPA Universität Stuttgart, POB 801140, 70511 Stuttgart,
Germany
e-mail: anne.juengert@mpa.uni-stuttgart.de

C. Große
Technische Universität München, Baumbachstraße 7,
81245 München, Germany

changes in the sound signals seen as changes in their frequency content. Additionally, the excitation force can be recorded using a dynamic force sensor implemented in the tip of the excitation hammer. Together, these procedures are known as Local Acoustic Resonance Spectroscopy (LARS).

2 Local Acoustic Resonance Spectroscopy

2.1 Measurement Principle

Non-destructive testing techniques using object resonance are well established in the testing of different kinds of materials [12]. For the investigation of metal and ceramic parts, acoustic resonance analyses are used. The objects are hit with a hard item and elastic waves are excited within the material. Due to the physical boundaries of the object, standing waves are formed and the object resonates in its normal modes. The air around the object starts to oscillate at the same frequencies and a sound is emitted. Flaws within the structure change the normal modes and therefore the sound. A change in the frequency content of the sound signal is recorded and defective parts can be quickly identified. This technique, however, only works for small parts with low sound attenuation. Due to the small size, the normal modes then lie in the audible frequency range. The low sound attenuation is required so that the waves can propagate through the part and standing waves are formed. For larger parts in the civil engineering, naval architecture, and aerospace industries, similar vibration analyses are used [3, 11]. The eigenfrequencies of these structures lie below the audible frequency range and have to be recorded using acceleration sensors. The vibrations can be excited using suitable sources or the vibrations excited during operation can be used. Damage within the structure change the eigenfrequencies and therefore can be detected. However, neither the acoustic resonance analysis nor the vibration analysis allows a localization of damages.

For damage localization in large structures made of fiber-reinforced plastic materials a related technique can be applied, such as LARS. During LARS, the structure is hit at a specific spot with a hard item and flaws such as voids underneath the surface lead to a change in the sound response of the structure. In general, the structures under investigation have normal modes that are very low in frequency and outside the audible frequency range. On one hand, this is caused by the size of the structures. On the other, the high sound attenuation of the materials affects the higher frequencies and higher modes are dampened quickly. Therefore, the excited sound is a very local response to the excitation and is not affected by the eigenmodes of the structure. The mechanism is explained in the next section.

LARS is mainly an advancement of standard coin-tapping tests [8, 16, 22, 30]. For LARS measurements it

is suggested to use an impulse hammer with an integrated force sensor for tapping. The ear of the observer is replaced by a microphone and a data recorder. The change in sound arises in a change of the frequency content of the recorded signal.

The measurements are taken at specific points along measurement lines or grids that allow the creation of two and three-dimensional images of the structure (the 3rd dimension is given by the half-widths of the excitation forces or frequency data).

2.2 Mechanics of LARS

Local acoustic resonance spectroscopy seems to be similar to resonance analyses, but the underlying physical mechanism is different.

The elastic properties of the test specimen play a major role, e.g. the bending stiffness

$$B' = E \cdot I \quad (1)$$

where E is Young's modulus and I the moment of inertia.

LARS can only be applied to materials with an intermediate bending stiffness, which is related to an intermediate E -modulus, and an intermediate sound attenuation. Soft materials like rubber or foam polymers exhibit a high damping of the impact sound and the propagation of elastic waves and are therefore not suitable. With very hard materials, the local character of the technique gets lost, because the bending amplitude will be smaller and covers a broader area of the test specimen.

However, the bending stiffness depends on the geometry of the structure. A structure that is thin relative to its length is easier to bend than a thick and short part. The technique therefore works very well on plate-like structures and is more sensitive to flaws near the surface.

Instead of the bending stiffness, the contact stiffness can be used to describe the mechanics of the technique. The contact stiffness depends not only on the properties of the investigated material, but also on the elastic properties of the hammer used and on the exciting force [21, 28].

According to Cawley and Adams [4], the contact endurance and the excited frequencies change if the contact stiffness changes. Following Hertz impact theory [13] the contact stiffness k_C is

$$k_C = \frac{3}{2} \left(\frac{16rE^*2}{9} \right)^{1/3} \cdot F^{1/3} \quad (2)$$

with $\frac{1}{E^*} = \frac{1-v_1^2}{E_1} + \frac{1-v_2^2}{E_2}$. E_i are the E -moduli, v the Poisson's ratios of the two materials and F the excitation force.

In addition to the sound signals, the force at the tip of the hammer is recorded with a dynamic force sensor. These are two independent parameters that are both linked to the contact stiffness.

2.3 Signal Analysis

According to Cawley and Adams and Hertz, the contact time increases if the contact stiffness between the hammer and the inspected structure decreases. This shows in the excitation force signal. Under ideal conditions the hammer impact produces a bell shaped curve at the force gauge in the hammer tip. The energy of the hammer impact is given as the area beneath the curve. The impact on a stiff surface (high contact stiffness) will lead to a high and narrow bell curve; the impact on a soft material (low contact stiffness) will produce a broader curve. Based on similar excitation forces, the area beneath the curves should be equal. Thus, the width of the bell curve depends on the contact stiffness. Flaws like delaminations or cavities decrease the contact stiffness and therefore lead to broader force signals.

To analyze the excitation forces, the contact time is calculated from the dynamic force sensor data. The half-width of the excitation force is determined for every excitation point. These half-widths can be linked to the measurement grid transformed into a 3-D color-coded or grayscale image.

The sound data from the microphone is converted to the frequency domain using a Fourier transform [2]. Changes in the contact stiffness lead to changes in the frequency content of the sound response and contain information about the condition of the structure at this specific location.

3 Investigation of Error Sources

During experimental measurements, errors occur for different reasons. The devices used are limited (e.g. by sampling rates and resolution of data acquisition) and peculiarities of some materials or components can affect the results. Therefore, it is important to examine the limits of new techniques to avoid misinterpretations.

3.1 Variation of the Excitation Force

According to Eq. (2), the contact stiffness, which is the cause of changes in the recorded signals, depends on the excitation force. If the excitation of the signal during LARS is done manually, the amplitude of the excitation force can vary. Therefore, it is necessary to investigate the effect of changing excitation forces versus the effects that are caused by material properties. To study these effects, an instrumented impulse hammer was used to manually tap a flawless glass fiber-reinforced polymer (GFRP) plate. Different hammer tips were used—hard and small tips made of steel and plastic and larger tips made from elastomers. In Fig. 1 the excitation signals for different excitations using a polyoxymethylene (POM) tip are shown. The left picture shows the recorded forces over time. The differences in the excitation force are visible in the different amplitudes of the signals. The smallest amplitude is more than three times smaller than the highest amplitude. Equation (2) predicts a change in the contact

Fig. 1 Signals recorded at the force gauge using a POM hammer tip and different excitation forces

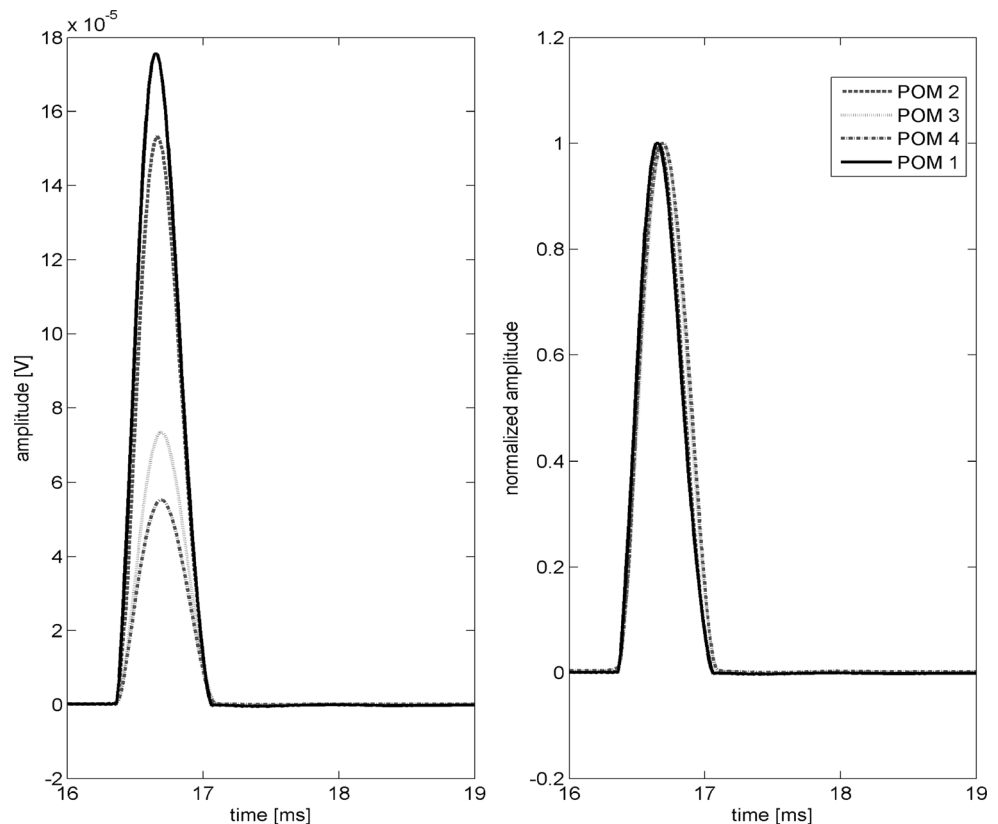
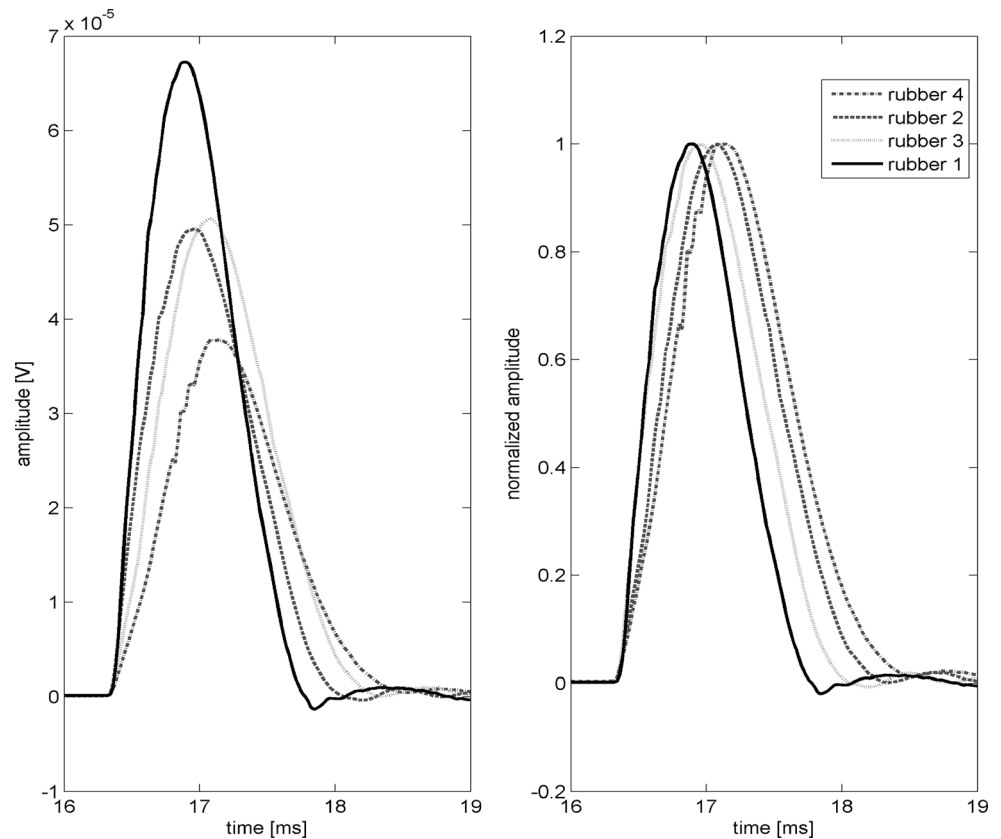


Fig. 2 Signals recorded at the force gauge using a elastomer hammer tip and different excitation forces



stiffness. This change should lead to a change in the contact time between hammer and GFRP plate. Therefore, it is necessary to look at the widths of the different excitation signals. The right picture in Fig. 1 shows the normalized excitation signals for a POM tip. It can be seen that differences in width are visible but small. If we take a closer (Table 1) look it can be seen that the half-widths of the curves vary by $50 \mu\text{s}$ from the lightest to the strongest tap. This difference is at least one order of magnitude smaller than differences caused by damages within GFRP. If a soft elastomer hammer tip is chosen instead of the POM tip, the differences in the half-width are much larger (Fig. 2). The measuring errors in the half-width determination are smaller if the hammer tip is harder. The POM tip is a suitable choice for the use at GFRP because steel tips could cause damage to the surface or the coating of the GFRP.

3.2 Investigation of Small Parts

In laboratory tests, investigated parts often are cutouts of bigger components and detached from their real environment. Therefore, tests have to be planned properly and the mounting of the test specimen plays a major role. It is sensible to mount the specimen such that the constraints mimic those of the part in an actual service environment.

In the following, a part of a fiber-reinforced plastic pipe is investigated. The pipe is usually used as a liner within

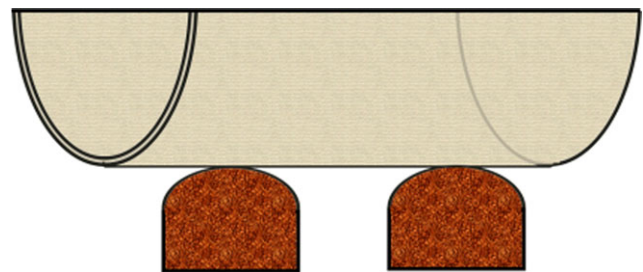


Fig. 3 Mounting of a pipe segment

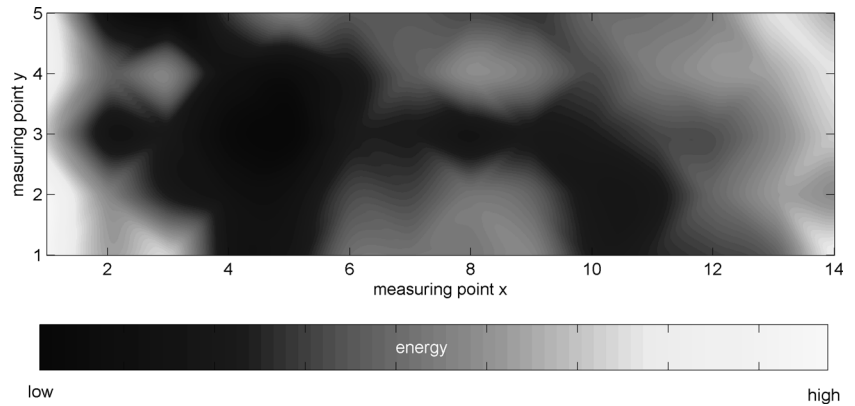
a larger stone/concrete pipe and is not under pressure. It is difficult to create similar mounting in the laboratory. Therefore, a pipe segment is mounted softly at two points of the test specimen to avoid the excitation of vibrations within the mounting. This scheme is shown in Fig. 3.

However, the analysis of the signals shows that the mounting still has an influence on the recorded data. The amplitude spectra of the sound signals at each measuring point were calculated and after normalization of the data, the energy of the signal was calculated as the area beneath the amplitude spectra. An energy value for each measuring point was evaluated and after a cubic interpolation the results are shown as grayscale images (Fig. 4). The mounting of the pipe segment is represented by the two dark areas of low energy. The soft mounting of the test specimen led

Table 1 Maximum amplitudes and corresponding half-width of the excitation with an impulse hammer

Material (line style in Figs. 1 and 2)	Maximum amplitude [μV]	Half-width [ms]
POM 1 (solid)	175 ± 4	0.035 ± 0.04
POM 2 (dashed)	153 ± 4	0.035 ± 0.04
POM 3 (dotted)	73 ± 2	0.039 ± 0.04
POM 4 (dash-dotted)	55 ± 2	0.040 ± 0.04
Elastomer 1 (solid)	67 ± 2	0.076 ± 0.04
Elastomer 2 (dashed)	51 ± 2	0.090 ± 0.04
Elastomer 3 (dotted)	50 ± 2	0.090 ± 0.04
Elastomer 4 (dash-dotted)	38 ± 1	0.096 ± 0.04

Fig. 4 Cumulated energy from the amplitude spectra of the sound signals recorded at a pipe segment



to a damping of the vibrations in the direct surrounding of the mounting. This effect was so strong that possible material defects could not be resolved. However, it is a good example for the locality of the technique. The mounting was localized very well using this technique.

If LARS is applied to smaller parts it is possible that the normal modes of test parts lie in the frequency range of the excited sound. In these cases the normal modes of the whole structure should be damped to conserve the local resonances only. Otherwise, the normal modes cover the local resonances and damage detection becomes difficult. Figure 5 shows the energy of the amplitude spectra within a certain frequency band of a flawed GFRP plate. The flaws were created using inserts of other materials. The flaws were localized using transillumination and thermography as Ref. [14]. The results of the analysis of the sound signals show a pattern which represents the normal modes of the plate comparable to Chladni figures [5, 26]. The pattern is visibly disturbed by a defect only at the lower edge ((0.10, 0) to (0.15, 0)). This was caused by a delamination in the material. Other damages are covered by the eigenmodes and could not be detected. Comparable patterns are visible in the other frequency bands as well.

3.3 Variation of Stress State

In practice, components often have to be investigated during production, before installation or built in as in-service

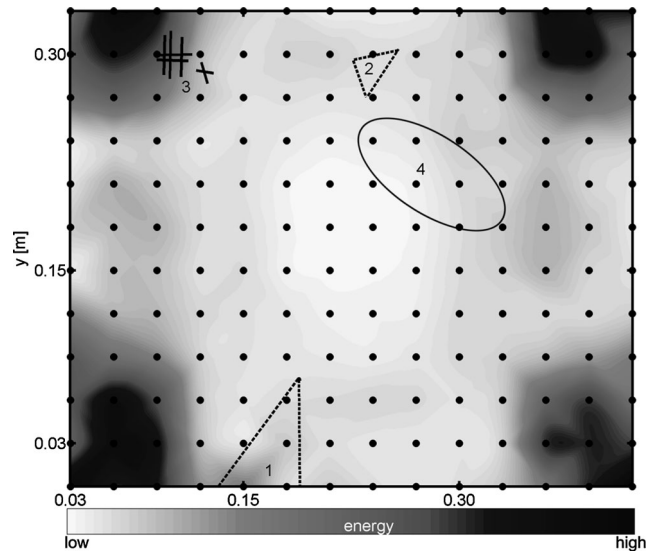
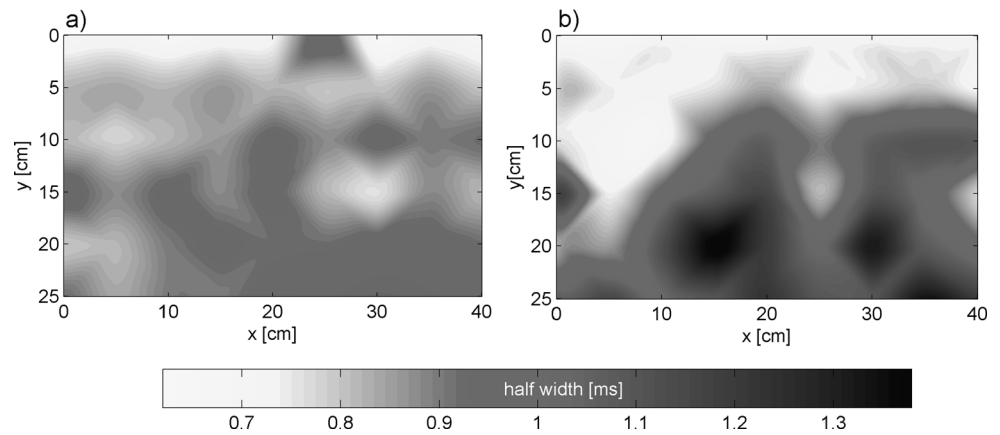


Fig. 5 Energy content of the sound signals within the frequency band from 120 to 135 Hz, recorded at a plate with flaws known from transillumination and thermography. The flaws are marked in the picture. Flaw 1 is a triangular delamination; flaw 2 and flaw 4 are inserts of other materials. The flaws marked with 3 only shows in the transillumination and are probably metal spikes. The transillumination and thermography results are shown in [14]

inspections. The stress state of the component is therefore variable. Whether the stress state of a component will affect the results of LARS was investigated. For this purpose,

Fig. 6 Half-width of excitation force at test field under (a) low stress and (b) high stress



a test field within a larger component was investigated in two different stress states. The investigated material was a sandwich composite containing plastic foam and GFRP.

During the first test, the component was bedded on the ground. A grid defining the test points was marked on the component. The stress within the test field (especially perpendicular to the sound excitation) was expected to be low. In the second test the component was fixed at one end and loaded with a static load, causing bending. Therefore, the stress within the test field was high.

In Fig. 6 the results of the analysis of the excitation forces is shown. The half-width of the excitation force was evaluated at each point of the test field and a grayscale image was generated. In Fig. 6(a) the data from the unstressed test field are shown; in Fig. 6(b) the data from the stressed test field can be seen using the same scale. As a result, the half-widths are smaller overall if the test field is under tension. The differences within the test field are still visible but are less distinctive. Thus, the contact stiffness is affected by the stress state of the component. High tension within the material decreases the resolution of the LARS measurements.

4 Application at Wind Turbine Blades

Rotor blades of wind turbines are lightweight structures with an aerodynamic shape comparable to the airfoils of gliders. The blades are mainly built of fiber-reinforced polymers. All highly stressed parts are realized as monolithic GFRP or CFRP laminates. The parts that are mainly responsible for the aerodynamic shape are built of sandwich materials containing wood (Balsa) or plastic foam. Possible flaws within the material are versatile and subject to current research [18, 19]. Wind turbine blades are difficult to investigate using non-destructive testing techniques. The thick GFRP laminates highly dampen elastic waves and the heat conduction is low. Besides, the sandwich areas are even more difficult to investigate with ultrasonic techniques. However, ultrasonic and thermographic techniques can be

adapted and applied to wind turbine blades to a certain extent [1, 29]. Ultrasound-Echo methods can be used to inspect the bond areas between different structural elements [9, 15, 20]. Techniques using ultrasonic guided waves are investigated as well [25]. Additionally, techniques for structural health monitoring in condition monitoring systems for existing blades are investigated [6, 17, 23]. In particular, LARS was developed to investigate the important structures of wind turbine blades to detect shallow delaminations, voids, and material changes.

4.1 Laboratory Test

A part of a damaged wind turbine blade was used to evaluate the LARS technique. The part (Fig. 7) was cut out near the flange of a wind turbine blade. The investigated surface covers 75 cm in the x -direction and 20 cm in the y -direction. Different material layers are visible in the cross section as well as a crack along the surface and a delamination of the different materials. A measurement grid with 5 cm spacing was used for LARS measurements.

The analysis of the excitation forces leads to Fig. 8(a). In the upper right corner of the test field an area of longer contact times (dark area) is observed. The delaminated layers are pressed together during the hammer impact. This leads to lower contact stiffness and a longer contact time. Smaller changes in contact time could be related to the structural changes due to material changes and material thicknesses. The dark area corresponds well to the cracked area, visible in the photo in Fig. 7. In Fig. 8(b) the results of the damaged area are plotted as an overlay onto the photo. It seems the delamination slightly overestimated by LARS. This is caused by the chosen measurement grid. The damage ends between two measurement points. The analysis uses an interpolation algorithm, so that the damage seems to be larger. The resolution of the analysis can be increased by decreasing the spacing between the measurement points. The analysis of the sound signals can be found in [14] and mainly confirm the results of this analysis.

Fig. 7 Photo of wind turbine blade part

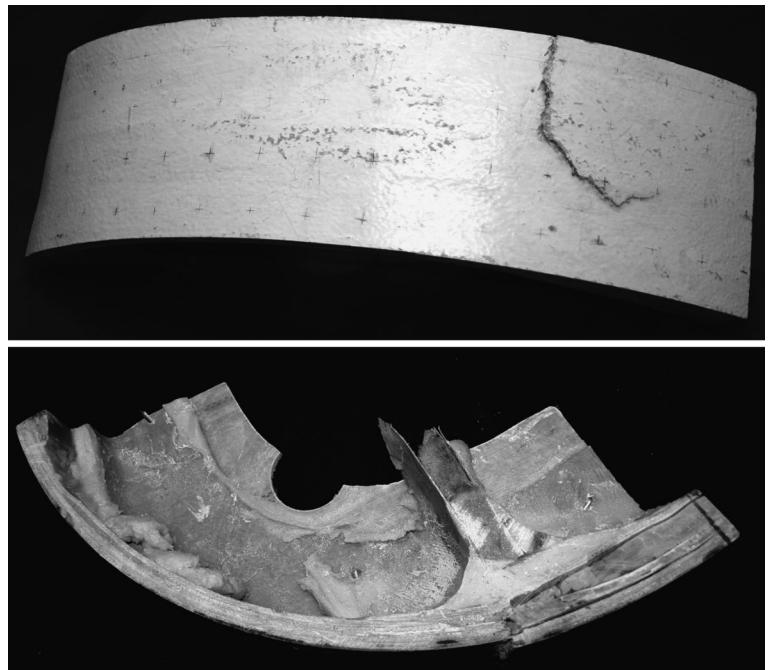
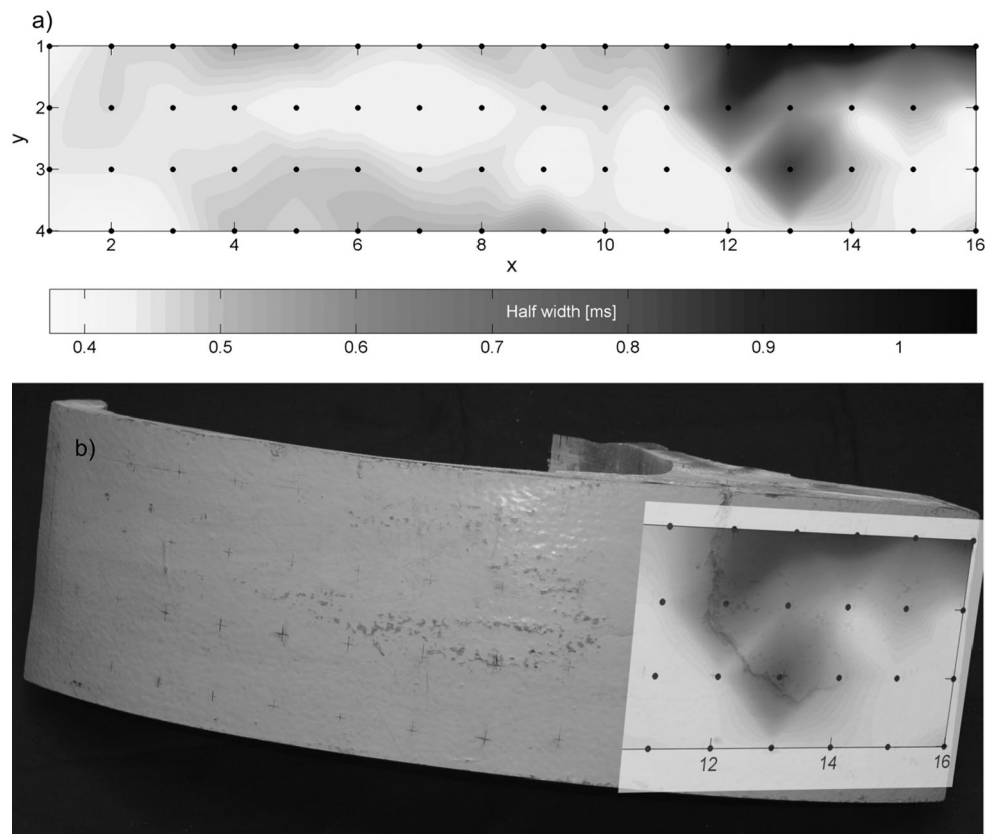


Fig. 8 (a) Half-widths of the excitation force recorded during a LARS at a part of a wind turbine blade; (b) overlay of the half-widths of the damaged area and a photo of the test part



4.2 Field Test

Field tests were performed on a wind turbine blade that had several visible defects and was scheduled for a dynamic load

test, monitored by vibration and sound emission analyses. Results of these other NDT techniques can be found in [27]. The wind turbine blade was delivered without a gel coat so some defects were already visible from outside the blade. An

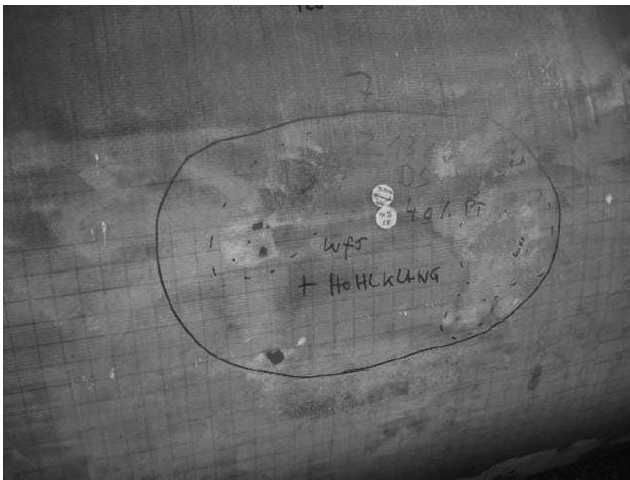


Fig. 9 Photo of the inspected area of a wind turbine blade. The *encircled area* corresponds to a delamination. The *dashed encircled areas* mark near surface material changes (degradation caused by ingress of moisture)

experienced rotor blade inspector (see acknowledgement) examined the turbine blade in advance by using a conventional coin tapping test and marking critical areas (Fig. 9). Due to the missing gel coat some structural details of the turbine blade can be seen through the GFRP. In the lower part there are small cubical inserts made of plastic foam. In the upper part the CFRP-belt is visible. The CFRP-belt is covered by a copper mesh which serves as lightning protection. The critical area is encircled. In the middle of the circle a hollow sound (supposedly a delamination) is marked with the word ‘Hohlklang’. Left and right from the delamination near surface, material changes can be seen as a snowflake-like pattern. They are encircled with a dashed line. The material changes are supposedly embrittlements or other degradations due to water inclusions [7].

Local acoustic resonance spectroscopy was applied along a staggered grid with a spacing of 5 cm covering the encircled area.

First, the excitation signals were analyzed. In Fig. 10 the half-widths of the excitation signals are plotted in 2D over the measurement grid. It can be seen that there is an area of enlarged half-width in the middle of the test field. The contact times between hammer and turbine blade are longer in this area than in the adjacent areas of the test field. This coincides with the delamination as marked by the inspector. To illustrate the similarities more clearly, Figs. 9 and 10 are combined in Fig. 11. The measured longer contact times between hammer and surface and the delamination clearly match. Also, the material changes near the surface (dashed line areas) affect the contact time.

After that, the recorded sound signals were analyzed. A fast Fourier transform was used to calculate the amplitude spectra of the sound signals. Two amplitude spectra of sound signals recorded in different areas of the test field are

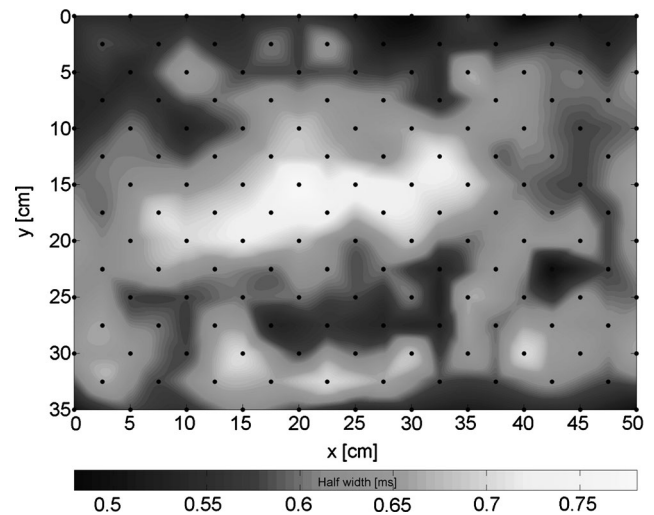


Fig. 10 Half-widths of the LARS at the test area

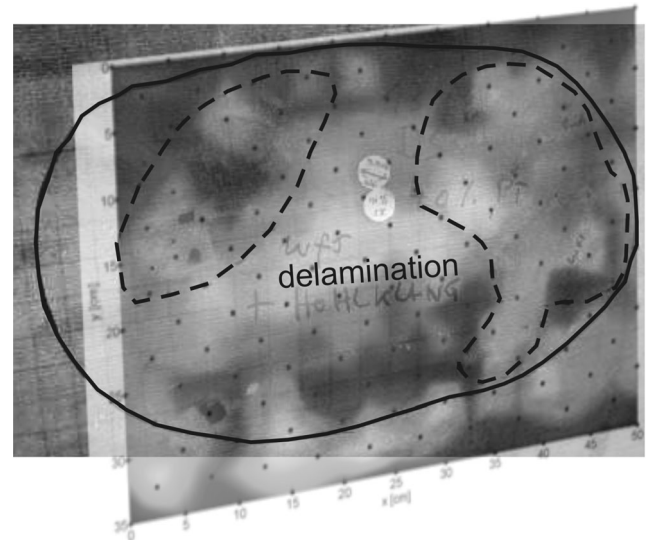


Fig. 11 Overlay of photo (Fig. 9) and results shown in Fig. 10. A delamination (hollow sound) is marked with the word “Hohlklang”. The delamination corresponds to the bright area (elongated contact times) in the middle. The *encircled areas with dashed lines* mark near surface material changes which overlay the elongated contact times of the delamination

shown in Fig. 12. The solid line belongs to a sound signal excited at the edge of the grid, where no damage was expected. The dashed line corresponds to sound excited in the center of the grid, where the delamination was marked. Differences in the frequency content of the two sound signals are visible. The spectral centroids [24] can be calculated for intact and damaged areas. In the intact area the main part of the sound energy (spectral centroid) is about 0.7 kHz and lower. The main part of the sound energy on the damaged areas lies above 0.9 kHz.

To compare the frequency content in the tested area, slices through the data-cube, containing the amplitude spec-

Fig. 12 Amplitude spectra of sound signals of a LARS recorded at different points of the wind turbine blade test field

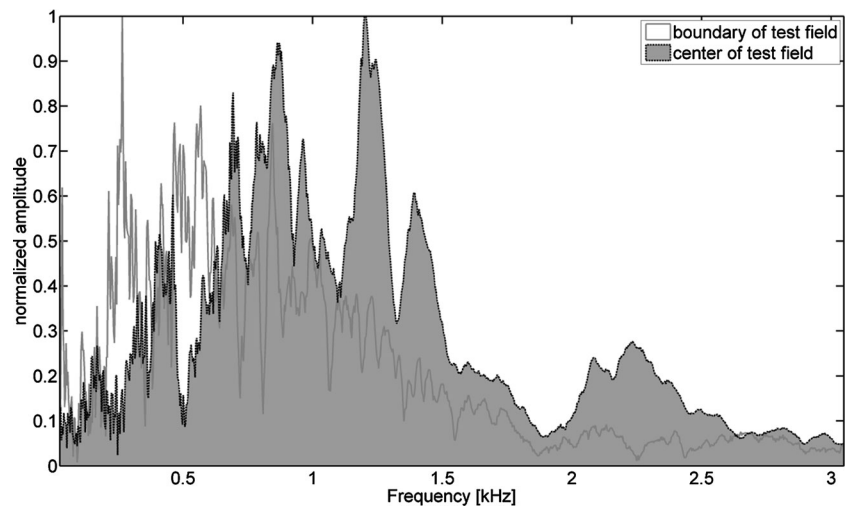
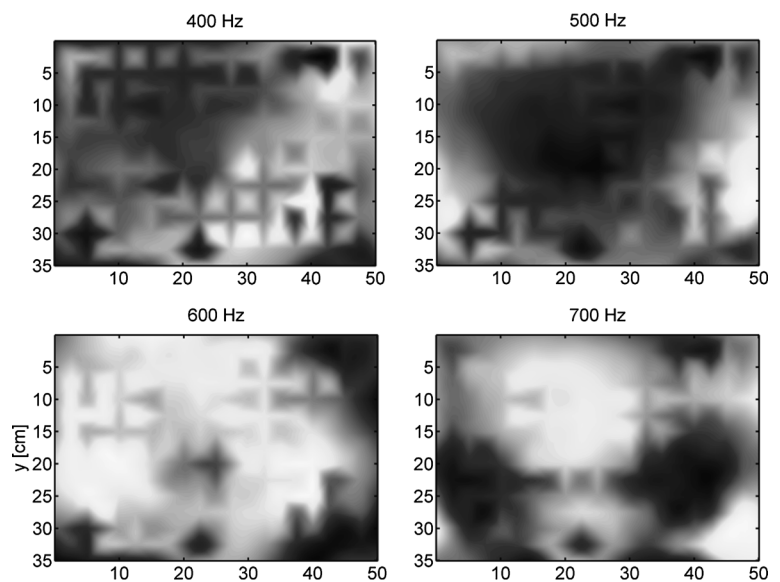


Fig. 13 Amplitude spectra slices at different frequencies; the amplitudes are grayscale. At 500 Hz an area of low amplitudes can be seen in the upper half of the figure. The same area shows high amplitudes at 700 Hz



tra along the measurement grid, were cut and are shown in Fig. 13. The slice at 500 Hz shows very low amplitudes (dark color) in the middle of the grid; the slices at 700 Hz and 800 Hz exhibit high amplitudes (light color) in the middle of the tested area. This is interpreted as the response to the delamination, which corresponds well to the delamination that was marked before by the inspector. These changes are not visible in other frequencies.

The analysis of the sound signals shows the delamination larger than the analysis of the excitation forces. The excitation signal is more affected by material changes near the surface than the sound signal. The grey spots around the marked delamination in the excitation signals (Fig. 11) follow the visible material changes in the first fiber layers. The sound signals does not seem to be affected by this material changes. Therefore, it is necessary to look at both signal types.

5 Discussion and Conclusions

Local acoustic resonance spectroscopy is an advancement of the tapping tests commonly used in the aerospace industry and in wind turbine blade inspections. The excitation force is recorded using a force gauge within the tip of a hammer, and the resulting sound is recorded using a microphone.

During the measurement process there is always uncertainty within the results. One source of uncertainty using LARS is the manual excitation of the sound signals. Changes in sound are caused by changes in the contact stiffness between hammer and test part. This contact stiffness depends to some degree on the excitation force. Within a lab test, the influence of this dependency was investigated. It could be shown that the differences in contact stiffness due to different excitation forces are measurable. Fortunately, they are one order smaller than the differences caused by

defects within the test part. However, for higher resolution measurements an automated excitation is required similar to the impacts used in impact-echo testing [10].

LARS works well on large components with intermediate sound attenuation. If small parts or cutouts of large components are to be investigated, problems may occur during the measurements. It is therefore recommended that the part be mounted such that the kinematic constraints and stress state match those of the part in a service environment. Due to the physical boundaries of smaller components, eigenmodes of the structure can be excited. It is required to dampen these normal modes to a certain degree using a suitable mounting of the test piece. But also the mounting of smaller components can affect the results as has been shown. The technique is particularly suitable for in-situ applications, and, to a lesser extent, small cutout parts. In addition, it was shown that the stress state of the investigated parts affects the results of a LARS test. This has to be kept in mind with moving components that change their location and stress state, e.g. wind turbine blades, and for parts that have to be inspected periodically. Furthermore, it was shown that the stress within the part should be kept low to allow higher resolution results.

Application of LARS to wind turbines showed that the method is a suitable technique for the detection of defects in the blades. In particular, delaminations and hollow areas can be detected using both contact time and sound response analysis. Because of its simplicity and insensitivity to weather conditions, the LARS method is particularly attractive for wind turbine blade testing. Moisture does not appear to affect the analysis, but temperature induced stress changes might affect the results. Further, it is a fast measuring technique and further automation is possible and will be explored for future applications to fiber-reinforced polymer constructions, including wind turbine blades. Another field of investigation will be the implementation of advanced analysis and signal processing algorithms to create images that could be interpreted by the rotor blade inspectors.

LARS is comparable to commercial equipment for bond testing (e.g. Mitsui Woodpecker) in aerospace industries. However, the Woodpecker analyses the contact times of the sound excitation only. LARS additionally provides the recording of the sound signals. The sound signals contain additional information and the combined analysis of excitation forces and sound signals could give information about the nature of flaws. This is especially important for the application to wind turbine blades, as damage here is more variable in size and origin, and has, in the case of aerospace materials, received less research attention.

There still is potential for improvement in the analysis of the sound signals. A systematic evaluation of the technique using artificial and realistic flaws with known dimensions and locations has to be done to distinguish different types of

flaws by their frequency content. It also is needed to identify the significant frequency ranges for different flaw types and rotor blade regions. Advanced techniques of signal processing and pattern recognition could also lead to automated damage detection.

Acknowledgements The authors thank the IZFP and the IMA Dresden for the possibility for conducting investigations of their test blade, Mr. Otto Lutz for the results of his inspection of the test blade and Mr. Sean Dugan for the kind revision of the text.

References

1. Aderhold, J., Meinschmidt, P., Brocke, H., Jüngert, A.: Rotor blade defect detection using thermal and ultrasonic waves. In: Proc. DEWI GmbH (Ed.): DEWEK 2008, Bremen (2008)
2. Bergland, G.D.: A guided tour of the fast Fourier transform. *IEEE Spectr.* **6**, 41–52 (1969)
3. Brownjohn, J.M.W., Magalhaes, F., Caetano, E., Cunha, A.: Ambient vibration re-testing and operational modal analysis of the Humber bridge. *Eng. Struct.* **32**(8), 2003–2018 (2010)
4. Cawley, P., Adams, R.D.: The mechanics of the coin-tap method of non-destructive testing. *J. Sound Vib.* **122**, 299–316 (1988)
5. Chladni, E.F.F.: *Die Akustik*. Breitkopf und Härtel, Leipzig (1802)
6. Ciang, C.C., Lee, J.-R., Bang, H.-J.: Structural health monitoring for a wind turbine system: a review of damage detection methods. *Meas. Sci. Technol.* **19**, 1–20 (2008)
7. Eslami, S., Taheri-Behrooz, F., Taheri, F.: Effects of aging temperature on moisture absorption of perforated GFRP. *Adv. Mater. Sci. Eng.* **7**, 1–7 (2012)
8. Georgeson, G., Lea, S., Hansen, J.: Electronic tap hammer for composite damage assessment. In: *NDE of Aging Aircr., Airpt. and Aerosp. Hardw.. Proc. SPIE*, vol. 2945, p. 328 (1996)
9. Gieske, J.H., Rumsey, M.A.: Nondestructive evaluation (NDE) of composite-to-metal bond interface of a wind turbine blade using an acousto-ultrasonic technique. Sandia report (1996)
10. Grosse, C., Wiggenhauser, H., Algernon, D., Schubert, F., Beutel, R.: *Impact-Echo-Stand der Technik und Anwendungen des Verfahrens*, Hefte des Deutschen Ausschusses für Stahlbeton DAFStb, vol. 565, pp. 17–24. Springer, Berlin (2006)
11. Haritos, N., Owen, J.S.: The use of vibration data for damage detection in bridges: a comparison of system identification and pattern recognition approaches. *Struct. Health Monit.* **3**(2), 141–163 (2004)
12. Hertlin, I.: *Acoustic Resonance Analysis*. NDT Compact and Understandable, vol. 5. Castell, Wuppertal (2003)
13. Hertz, H.: Über die Berührung fester elastischer Körper. *J. Reine Angew. Math.* **92**, 156–171 (1881)
14. Jüngert, A.: *Untersuchung von GFK-Bauteilen mit akustischen Verfahren am Beispiel der Rotorblätter von Windenergieanlagen*. Dissertation, Universität Stuttgart, Stuttgart (2010)
15. Jüngert, A., Grosse, C.U.: Inspection techniques for wind turbine blades using ultrasound and sound waves. In: *Intern. Symp. Non-Destructive Testing in Civil Engineering (NDT-CE)*, pp. 625–632 (2009). ISBN 978-2-7208-2542-5
16. Kim, S.J.: Damage detection in composite laminates using coin-tap method. In: *Proc. Acoustics '08*, Paris, pp. 405–409 (2008)
17. Kristensen, O.J.D., McGugan, M., Sendrup, P., Rheinländer, J., Rusborg, J., Hansen, A.M., et al.: *Fundamentals for Remote Structural Health Monitoring of Wind Turbine Blades—a Preproject Annex E-Full-Scale Test of Wind Turbine Blade, Using Sensors and NDT*. RISO National Laboratory, Roskilde, Denmark (2002)

18. Mandell, J.F., Cairns, D.S., Samborsky, D.D., Morehead, R.B., Haugen, D.J.: Prediction of delamination in wind turbine blade structural details. *J. Sol. Energy Eng.* **125**, 522–530 (2003)
19. Mandell, J.F., Samborsky, D.D., Wang, L.: New fatigue data for wind turbine blade materials. *J. Sol. Energy Eng.* **125**, 506–514 (2003)
20. Mattei, C., Dahren, M.: Advanced ultrasonic NDT techniques for wind turbine blade inspection. *JEC Compos. Mag.* **46**, 58–60 (2009)
21. Maw, N., Barber, J.R., Fawcett, J.N.: The oblique impact of elastic spheres. *Wear* **38**, 101–114 (1976)
22. Mitsuhashi, K., Jyomuta, C., Oka, F., Nishikawa, H.: Method and apparatus for impact-type inspection of structures. Patent publication number: 05,048,320 (1989)
23. Nijssen, R.P.L.: Fatigue life prediction and strength degradation of wind turbine rotor blade composites. Sandia, Montana State University (SAND2006-7810P) (2007)
24. Peeters, G.: A large set of audio features for sound description (similarity and classification) in the CUIDADO project. Cuidado project report, IRCAM, Paris (2004)
25. Raisutis, R., Jasiuniene, E., Zukauskas, E.: Ultrasonic NDT of wind turbine blades using guided waves. *Ultrasound* **63**(1), 7 (2008)
26. Rayleigh, J., Lord, W.S.: On the calculation of Chladni's figures for a square plate. *Philos. Mag. Ser. 6* **22**(128), 225–229 (1911)
27. Schulze, E., Schubert, L., Frankenstein, B.: Monitoring of a wind turbine rotor blade with acousto ultrasonics and acoustic emission techniques during a full scale fatigue test. In: Proc. of the 5th European Workshop on Structural Health Monitoring, Sorrento, Naples, Italy, 28.6.–4.7.2010, pp. 1229–1234 (2010)
28. Shi, X., Polycarpou, A.A.: Measurement and modeling of normal contact stiffness and contact damping at the meso scale. *J. Vib. Acoust.* **127**, 52–60 (2005)
29. Sutherland, H.J., Beattie, A., Hansche, B.: The application of non-destructive techniques to the testing of a wind turbine blade. Sandia report (1994)
30. Wu, H., Siegel, M.: Correlation of accelerometer and microphone data in the “coin tap test”. *IEEE Trans. Instrum. Meas.* **49**(3) (2000)